Generalized and Average Likelihood Ratio Testing for Post Detection Integration

Giovanni Emanuele Corazza, *Member, IEEE,* and Raffaella Pedone, *Student Member, IEEE*

Abstract

In the context of spread spectrum communications, this paper investigates the use of Likelihood Ratio Testing techniques for the design of Post Detection Integration (PDI) methods for code acquisition in the presence of phase and frequency uncertainty. The proposed methods are derived as theoretical and pragmatic alternatives to the conventional approach based on non-coherent integration, which would be optimal in the absence of frequency uncertainty. Two competing alternatives are introduced to handle the unknown frequency error, respectively based on the generalized and average likelihood ratio tests, and identified as Generalized PDI (GPDI) and Average PDI (APDI). The GPDI vs. APDI trade-off is far from trivial and leads to numerous interesting insights, particularly with respect to the impact on performance of the frequency offset entity. Performance is also contrasted to that of conventional PDI techniques, i.e. non-coherent and differential PDI, to reveal significant gains in favor of the proposed methods.

Index Terms

Spread Spectrum, Code Acquisition, Post Detection Integration, Frequency Error, Likelihood Ratio Test.

I. Introduction

In recent years, the set of applications of Spread Spectrum (SS) techniques has witnessed a phenomenal growth, in view of the intrinsic and beneficial characteristics such as the robustness against intentional interference, interception and multipath; high accuracy for time delay measurements; efficient multiple access capability based on code division (CDMA) [1], [2], [3]. It can be stated that the role of SS techniques is not only undeniable in the military arena, but is now recognized as a cornerstone in the commercial market, both for navigation/positioning services and for present and future generations of cellular networks.

However, all of the advantages possessed by SS transmission can only be exploited after code synchronization is successfully achieved [2]. The alignment between the transmission spreading code and the locally generated sequence is in fact the necessary prerequisite for correct data demodulation and decoding. Code synchronization is typically split into two cascaded phases. The first phase is identified as code acquisition and provides the coarse code epoch estimate [4], [5]. The second step is code tracking, which produces continuous fine alignment between the transmitted and local code. Code acquisition is based on the discretization of the usually immense uncertainty region into cells or *hypotheses*, so that the complex problem of code epoch estimation is transformed into a simpler detection problem. We identify as the H_1 *hypothesis* each synchronous cell corresponding to correct alignment, while the H_0 *hypothesis* identifies all misaligned cells. Thus, code acquisition can be treated as a binary decision problem to discriminate between H_1 and H_0 [6]. The pseudonoise (PN) sequence employed in transmission is typically characterized by large in-phase and low out-of-phase autocorrelation, and thus the detection is driven by the search for the correlation peak between the received signal and the local PN sequence.

The extremely low signal-to-noise (SNR) ratio (normally in the range from -10 to -20 dB) characterizing the SS signal before despreading makes it typically unfeasible to anticipate carrier recovery with respect to code synchronization. Thus, code acquisition is practically always the first operation to be performed, and must be designed taking into account the unavoidable phase and frequency uncertainty affecting the received signal. In particular, a frequency error can be present due to transmit/receive oscillators mismatch and possible terminal motion. Besides the additional angle rotation, the frequency offset introduces an energy degradation which makes it impracticable to perform coherent correlation over the entire PN sequence period. In order to alleviate this degradation, a windowing technique is employed [7], limiting coherent correlation over an appropriately dimensioned sub-sequence [8], [9], [10], and introducing Post Detection Integration (PDI) on the collected partial outputs. PDI improves the SNR before detection notwithstanding the noise-signal cross terms introduced by the necessary non linearities.

A pragmatic approach has been adopted for more than thirty years in practical systems to solve code detection in phase and frequency uncertainty, consisting in the extension of the application of the energy detector, which is actually the optimal solution when there is no frequency offset [6]. This practical solution corresponds in essence to block non-coherent detection (Non-Coherent PDI - NCPDI) [7], [11]. A possible alternative to this approach is represented by Differential PDI (DPDI) [12], [13], [14], [15], which can outperform NCPDI in the presence of large frequency errors due to the reduced noise enhancement.

The main objective of this paper is to derive quasi-optimal PDI schemes through the application of a

theoretical approach in resolving the frequency error uncertainty. In particular, the likelihood ratio testing (LRT) approach is applied for the detection problem under evaluation, and two different solutions are identified. The first is based on the generalized LRT [6] and is referred to as Generalized PDI (GPDI). The second eliminates the uncertainty by averaging out the unknown frequency offset, and the resulting solution is identified as Average PDI (APDI). The study is here developed for the fundamental Additive White Gaussian Noise (AWGN) channel, and its extension to fading channels is a matter for further future work. Also, pilot-aided synchronization is considered, as customary in the majority of SS systems, but consideration of data uncertainty is another interesting path for additional research efforts.

The performance of the proposed solutions is compared in terms of Receiver Operating Characteristics (ROCs) to find out possible performance improvements. The GPDI vs. APDI trade-off is far from trivial and leads to numerous interesting insights. In particular, GPDI is the most robust solution when frequency offsets are large, while APDI becomes the smartest approach for fine offsets. The classic NCPDI and DPDI approaches can always be outperformed, at the price of a moderate complexity increase.

Besides the application to code acquisition for SS systems, the proposed methods can be usefully exploited to solve similar synchronization issues in other scenarios. For example, a fruitful field of application is in the design of frame acquisition procedures for time division multiple access systems, e.g. for the forthcoming DVB-S2 standard [16].

The paper is organized as follows. Section II describes the system model, while Section III provides the analytical procedure to derive the likelihood ratio test for both generalized and average strategies. Section IV addresses the analytical characterization of the performance, and Section V shows the numerical results. Finally, in Section VI the paper conclusions are drawn.

II. System Model

The acquisition sub-system is the typical pilot-aided code acquisition scheme [5], [11], shown in Fig. 1, where the PDI block is purposely left generic, its design being the objective of the paper. We consider a real-valued spreading sequence, with no loss in generality. The received signal in AWGN under the hypotheses H_1 (pilot present) and H_0 (no pilot) can be modelled respectively as

$$r(t) = \begin{cases} \mathrm{H}_1: & p(t) + n(t) \\ \mathrm{H}_0: & n(t) \end{cases} \tag{1}$$

where $p(t)$ is the pilot tone signal, and $n(t)$ is stationary AWGN with power spectral density $N_0/2$. The model for H_0 corresponds to neglecting the possible presence of autocorrelation side-lobes. The pilot

tone signal can be written as:

$$p(t) = \sqrt{2P}\, a(t-\tau)\cos[2\pi(f_0+\Delta f)t+\theta] \tag{2}$$

where P is the pilot power, f_0 is the nominal carrier frequency, τ is the unknown delay, Δf is the unknown frequency offset, and θ is the unknown carrier phase. Finally, $a(t)$ is the pseudo-noise sequence (PNS), which can be written as

$$a(t) = \sum_{k=-\infty}^{+\infty} a_{|k|_{L_S}}\, g(t-kT_c) \tag{3}$$

where L_S is the PNS length, $g(t)$ is the unit-energy chip pulse and T_c is the transmission code chip period. The received signal undergoes in-phase and quadrature (IQ) down-conversion, chip matched filtering, sampling, and despreading. Either active or passive correlation can be considered to optimize the complexity vs. delay trade-off. In the latter case, despreading is performed through PNS matched filtering. As explained in the Introduction, PNS correlation is performed coherently over a sub-sequence of M samples. This despreading operation is normalized by a factor $\sqrt{M}$, so that the IQ variates at its output are Gaussian distributed with a variance $\sigma^2 = N_0/2$. The optimal selection of the coherent integration length, M, depends on the (maximum) frequency error and is dependent on the specific PDI block design [8]. A rapid sub-optimum dimensioning rule, which equally apply to all PDI schemes, is reported in [9], [10].

In general, chip sampling occurs in the presence of a timing offset, bringing in two effects: a loss in useful signal energy, and the onset of inter-chip interference. Both effects could be included in the analysis, but only introduce obscuring mathematical details and no further insight. Therefore, for the sake of enucleating the essential facts, we assume ideal chip sampling in the following. The complex despread samples under H_1 can be written as

$$x_k = A(\Delta f)e^{j\theta}e^{j2\pi k\Delta f T} + n_k = s_k(\Delta f)e^{j\theta} + n_k \qquad \text{for} \quad k = 1,\ldots,L \tag{4}$$

where L is the PDI length, such that $L \cdot M = L_S$ and

$$A(\Delta f) = \sqrt{PT}\,\mathrm{sinc}(\Delta f T) \tag{5}$$

$$s_k(\Delta f) = A(\Delta f)e^{j2\pi k\Delta f T} \tag{6}$$

where T is the coherent integration time window, i.e. $T = MT_c$.

Observing the despread complex symbol x_k, we note that the frequency error induces an additional angle rotation and an energy degradation quantified by $\mathrm{sinc}^2(\Delta f T)$. This attenuation justifies the necessity

to limit coherent integration, so that T is significantly smaller than $1/\Delta f_{\max}$, where $\Delta f_{\max}$ is the maximum frequency offset, to have $\mathrm{sinc}^2(\Delta f T) \approx 1$. Introducing vectorial notation, let

$$\bar{x} = [\ x_1 \quad \cdots \quad x_L\ ]^T \tag{7}$$

$$\bar{s}(\Delta f) = [\ s_1(\Delta f) \quad \cdots \quad s_L(\Delta f)\ ]^T \tag{8}$$

$$\bar{n} = [\ n_1 \quad \cdots \quad n_L\ ]^T \tag{9}$$

where $[\cdot]^T$ indicates the transpose operation, so that equation (4) can be rewritten as

$$\bar{x} = \bar{s}(\Delta f)e^{j\theta} + \bar{n} \tag{10}$$

III. Likelihood Ratio Testing

The probability density functions (pdf's) of $\bar{x}$ under H_1 and H_0, given the unknown Δf and θ, are easily shown to be, respectively

$$p(\bar{x}|H_1, \Delta f, \theta) \quad = \quad \frac{1}{(2\pi\sigma^2)^L} \exp\left\{ - \frac{\|\bar{x} - \bar{s}(\Delta f)e^{j\theta}\|^2}{2\sigma^2} \right\} \tag{11}$$

$$p(\bar{x}|H_0) = \frac{1}{(2\pi\sigma^2)^L}\ \exp\left\{ - \frac{\|\bar{x}\|^2}{2\sigma^2} \right\} \tag{12}$$

The likelihood ratio (LR) is therefore

$$\ell(\Delta f, \theta) \quad = \quad \frac{p(\bar{x}|H_1, \Delta f, \theta)}{p(\bar{x}|H_0)} = \exp\left\{ - \frac{\|\bar{s}(\Delta f)e^{j\theta}\|^2}{2\sigma^2} \right\} \exp\left\{ \frac{\mathrm{Re}\{\bar{x} \cdot \bar{s}^*(\Delta f)e^{-j\theta}\}}{\sigma^2} \right\} \tag{13}$$

$$= \quad \exp\left\{ - \frac{LA^2(\Delta f)}{2\sigma^2} \right\} \exp\left\{ \frac{\mathrm{Re}\{\bar{x} \cdot \bar{s}^*(\Delta f)e^{-j\theta}\}}{\sigma^2} \right\} \tag{14}$$

where we neglected all irrelevant constants. Note that $\ell(\Delta f, \theta)$ contains as usual the energy and correlation terms, both of which are functions of the frequency error. The goal is to derive a theoretical LRT independent of the phase and frequency uncertainty. To this aim, the first step is to eliminate the dependence on the unknown phase, which is assumed to be invariant over the entire correlation span. Letting θ be a random variable (rv) with uniform pdf,

$$p_\theta(\theta) = \frac{1}{2\pi}, \qquad \theta \in [-\pi, \pi[\tag{15}$$

and averaging over its domain, the resulting average likelihood ratio (ALR) is

$$\ell(\Delta f) \quad = \quad \int_{-\pi}^{\pi} \ell(\Delta f, \theta) p_\theta(\theta) d\theta = \exp\left\{ - \frac{LA^2(\Delta f)}{2\sigma^2} \right\} I_0\left(\frac{1}{\sigma^2} \left| \bar{x} \cdot \bar{s}^*(\Delta f) \right| \right) \tag{16}$$

where $I_0(\cdot)$ denotes the zero-order modified Bessel function of the first kind. Let the average log-likelihood ratio (ALLR) be defined as

$$\Lambda(\Delta f) = \ln \ell(\Delta f) = -\frac{LA^2(\Delta f)}{2\sigma^2} + \ln I_0\left(\frac{1}{\sigma^2}\left|\bar{x}\cdot\bar{s}^*(\Delta f)\right|\right) \tag{17}$$

Using the well-known approximation for small arguments of the logarithmic zero-order modified Bessel function $\ln I_0(x) \approx \frac{x^2}{4}$, yields

$$\Lambda(\Delta f) \simeq -\frac{LA^2(\Delta f)}{2\sigma^2} + \frac{1}{4\sigma^4}\left|\bar{x}\cdot\bar{s}^*(\Delta f)\right|^2 \tag{18}$$

Substituting (6) into (18) and rearranging, it follows

$$\Lambda(\Delta f) = \frac{A^2(\Delta f)}{4\sigma^4}\left\{\left|\sum_{k=1}^{L} x_k e^{-j2\pi k\Delta f T}\right|^2 - 2L\sigma^2\right\} \tag{19}$$

It is interesting to note that, if the frequency error vanishes, $\Delta f \to 0$, then the ALLR reduces to

$$\Lambda(\Delta f \to 0) = \frac{A^2(0)}{4\sigma^4}\left|\sum_{k=1}^{L} x_k\right|^2 \tag{20}$$

which simply corresponds to performing coherent integration over the total observation period $LT = LMT_c$, with a final IQ square and sum. This is the known and expected solution which is optimal if and only if there is no frequency error.

Exploiting the fact that we have limited the coherent integration span to ensure $\mathrm{sinc}^2(\Delta f T) \approx 1$, then

$$A^2(\Delta f_{\max}) \simeq PT \tag{21}$$

In this case, the multiplicative term in (19) is a constant and can be incorporated into the threshold. Finally, we can rewrite the ALLR as

$$\Lambda(\Delta f) = \left|\sum_{k=1}^{L} x_k e^{-j2\pi k\Delta f T}\right|^2 \tag{22}$$

The next step, consisting in the elimination of the frequency uncertainty, is handled in two different ways, leading to the generalized and average LRTs.

A. Generalized likelihood ratio testing

Let Δf be modelled as a deterministic unknown parameter. We can form the generalized likelihood ratio as

$$\Lambda = \max_{\Delta f}\Lambda(\Delta f) = \max_{\Delta f}\left|\sum_{k=1}^{L} x_k e^{-j2\pi k\Delta f T}\right|^2 \tag{23}$$

It is worthwhile noting that solving directly (23) would amount to finding the Maximum Likelihood (ML) estimate of Δf before detecting the presence of the signal. However, being the experienced SNR typically very low, this estimation procedure is rarely feasible with the desired quality, due to the high probability of outliers. Moreover, the computation of $\frac{d\Lambda(\Delta f)}{d\Delta f} = 0$ does not lead to any simple results. A more appealing solution may be found by proceeding as in the following. Start by rewriting (22) as

$$\Lambda(\Delta f) \quad = \quad \sum_{k=1}^{L}\sum_{h=1}^{L} x_k x_h^* e^{-j2\pi(k-h)\Delta f T} \tag{24}$$

Our proposed methods stem from the observation that these L^2 terms can be grouped according to the angle rotation as follows

$$\begin{aligned}\Lambda(\Delta f) \quad &= \quad \sum_{k=1}^{L} x_k x_k^* + 2\mathrm{Re}\left\{\sum_{k=2}^{L} x_k x_{k-1}^* e^{-j2\pi\Delta f T}\right\} + 2\mathrm{Re}\left\{\sum_{k=3}^{L} x_k x_{k-2}^* e^{-j2\pi 2\Delta f T}\right\} + \cdots + \\ &+ \quad 2\mathrm{Re}\left\{\sum_{k=n+1}^{L} x_k x_{k-n}^* e^{-j2\pi n\Delta f T}\right\} + \cdots + 2\mathrm{Re}\left\{x_L x_1^* e^{-j2\pi(L-1)\Delta f T}\right\}\end{aligned} \tag{25}$$

which we rewrite concisely as

$$\Lambda(\Delta f) = \Lambda_0 + \sum_{n=1}^{L-1} \Lambda_n(\Delta f) \tag{26}$$

where

$$\Lambda_0 = \sum_{k=1}^{L} |x_k|^2 \tag{27}$$

corresponds to the classic NCPDI scheme, which evidently is not affected by the frequency offset, and

$$\Lambda_n(\Delta f) = 2\mathrm{Re}\left\{\sum_{k=n+1}^{L} x_k x_{k-n}^* e^{-j2\pi n\Delta f T}\right\} \tag{28}$$

Introducing for convenience the complex number

$$y_n = |y_n| e^{j\phi_n} = \sum_{k=n+1}^{L} x_k x_{k-n}^* \tag{29}$$

we can rewrite (28) as

$$\Lambda_n(\Delta f) \quad = \quad 2\mathrm{Re}\left\{|y_n| e^{j\phi_n} e^{-j2\pi n\Delta f T}\right\} = 2|y_n|\cos(\phi_n - 2\pi n\Delta f T) \tag{30}$$

Having abandoned the hope to maximize (26) directly, the idea is to settle for a maximization of the single terms (30). This does not lead to a single estimate of Δf, which however was not the objective in the first place; rather, this yields a simple and effective detection rule which we will show to outperform

previously known solutions. Considering a single $\Lambda_n(\Delta f)$ term, it is immediate to solve the maximization problem

$$\Lambda_n^{\mathrm{G}} = \max_{\Delta f} \Lambda_n(\Delta f) \tag{31}$$

In fact,

$$\left[\frac{d\Lambda_n(\Delta f)}{d\Delta f}\right]_{\Delta f=\hat{\Delta f}_n} = 0 \quad \Longrightarrow \quad \hat{\Delta f}_n = \frac{\phi_n}{2\pi nT} \tag{32}$$

and the generalized ALLR term becomes

$$\Lambda_n^{\mathrm{G}} = 2\left|\sum_{k=n+1}^{L} x_k x_{k-n}^*\right| \tag{33}$$

Repeating this procedure for all $\Lambda_n(\Delta f)$ terms, and substituting into (26), yields a test which is independent of the frequency offset value, namely

$$\Lambda^{\mathrm{G}} = \sum_{n=0}^{L-1} \Lambda_n^{\mathrm{G}} \underset{\hat{H}_0}{\overset{\hat{H}_1}{\gtrless}} \xi \tag{34}$$

where ξ is the detection threshold, and

$$\begin{aligned}
\Lambda_0^{\mathrm{G}} &= \Lambda_0 = \sum_{k=1}^{L} |x_k|^2 && \text{NCPDI} \\
\Lambda_1^{\mathrm{G}} &= 2\left|\sum_{k=2}^{L} x_k x_{k-1}^*\right| && \text{DPDI} \\
&\vdots && \\
\Lambda_n^{\mathrm{G}} &= 2\left|\sum_{k=n+1}^{L} x_k x_{k-n}^*\right| && n\text{-Span DPDI} \\
&\vdots && \\
\Lambda_{L-1}^{\mathrm{G}} &= 2\,|x_L x_1^*| && (L-1)\text{-Span DPDI}
\end{aligned} \tag{35}$$

The solution provided by (34) is referred to as the GPDI[Λ] system, which compares the total likelihood ratio Λ^{G}, composed by L terms, with the detection threshold. While we already noted that Λ_0 is NCPDI, the second term Λ_1^{G} corresponds to the DPDI scheme [12] multiplied by a factor of 2, and both are particular terms of the complete GPDI[Λ]. These two terms are linearly combined with several additional terms, which are similar to DPDI, but they take as a reference the n-th past symbol instead of the immediate predecessor. This suggests to indicate as n-Span DPDI the generic additional PDI term, as reported in (35). Fig. 2(a) shows the detector block diagram for Λ_0, while in Fig. 2(b) the generic n-Span DPDI detector is reported. Finally, Fig. 3(a) shows the block diagram for the total GPDI[Λ] system.

Notice that, as we will show in the numerical analysis, the law of diminishing returns applies, i.e. the gain obtained by adding the n-Span DPDI terms becomes smaller and smaller with increasing n. In addition, the larger n the more stringent becomes the assumption of constant channel-induced phase rotation, which is at the basis of the n-Span terms operation. For these reasons, it may be wise in practice to arrest the sum in (34) before $n=L-1$. Therefore, we introduce the following notation

$$\Lambda^{\mathrm{G}}(m) = \sum_{n=0}^{m-1} \Lambda_n^{\mathrm{G}} \tag{36}$$

to indicate the partial likelihood ratio obtained by summing only $m \leq L$ contributions. The PDI scheme implementing (36) is referred to as GPDI$[\Lambda(m)]$. A very appealing particular case is GPDI$[\Lambda(2)]$ achieved by summing NCPDI and DPDI only, i.e.

$$\Lambda^{\mathrm{G}}(2) = \Lambda_0 + \Lambda_1^{\mathrm{G}} \tag{37}$$

The simulation campaign will confirm that this simplified case represents a good trade-off between acquisition performance and complexity. Note that if the sum in (26) is truncated as

$$\Lambda(\Delta f) = \Lambda_0 + \Lambda_1(\Delta f) \tag{38}$$

the maximization with respect to Δf leads rigorously to (37), and a single frequency offset estimate is also obtained as a by-product. Finally, note that the double weight of DPDI with respect to NCPDI in (37) has been confirmed to be optimal also by numerical simulation [17].

B. Average likelihood ratio testing

In this case Δf is assumed to be a rv with uniform distribution, i.e.

$$p_{\Delta f}(\Delta f) = \frac{1}{2\Delta f_{\max}}, \quad \Delta f \in [-\Delta f_{\max}, \Delta f_{\max}] \tag{39}$$

Averaging with respect to this statistical distribution for the frequency offset is the classic approach for eliminating the dependence from Δf, as done for example in [18]. As we will show later, this approach is inferior to GPDI when $\Delta f_{\max}$ is large. The reason lies in the fact that in most practical cases Δf is an unknown deterministic parameter and the uniform pdf model does not represent it well unless $\Delta f_{\max}$ is small. In fact, this method becomes very useful and possibly the best for fine offsets.

The average should in general be taken on the LR and not on the logarithmic LR (LLR), because the non linearity of the logarithm precludes the possibility to exchange the order of the operations. Surprisingly, the interesting result is that the same practical solution is obtained in both ways, i.e. the

final likelihood ratio test is identical, as we prove in the following. Starting from the ALR in equation (16), we approximate the zero order modified Bessel function as $I_0(x) \simeq 1 + x^2/4$

$$\ell(\Delta f) \simeq \exp\left\{-\frac{LA^2(\Delta f)}{2\sigma^2}\right\}\left(1+\frac{1}{4\sigma^4}\left|\bar{x}\cdot\bar{s}^*(\Delta f)\right|^2\right) \tag{40}$$

Averaging with respect to Δf, substituting (6), and introducing the assumption (21) of limited energy loss, we obtain

$$\ell^{\mathrm{A}} = \frac{PT}{8\sigma^4\Delta f_{\max}}\exp\left\{-\frac{LPT}{2\sigma^2}\right\}\left(\frac{8\sigma^4\Delta f_{\max}}{PT}+\int_{-\Delta f_{\max}}^{\Delta f_{\max}}\left|\sum_{k=1}^{L}x_k e^{-j2\pi k\Delta f T}\right|^2 d\Delta f\right) \tag{41}$$

Neglecting irrelevant multiplicative and additive constants, the following likelihood ratio is statistically sufficient

$$\ell^{\mathrm{A}} = \frac{1}{2\Delta f_{\max}}\int_{-\Delta f_{\max}}^{\Delta f_{\max}}\left|\sum_{k=1}^{L}x_k e^{-j2\pi k\Delta f T}\right|^2 d\Delta f \tag{42}$$

Now, the same result is obtained by taking the average of the ALLR in (22), i.e.

$$\Lambda^{\mathrm{A}} = \int_{-\Delta f_{\max}}^{\Delta f_{\max}}\Lambda(\Delta f)p_{\Delta f}(\Delta f)d\Delta f = \ell^{\mathrm{A}} \tag{43}$$

The explanation for this apparently anomalous result comes from two facts: first, the relevant term is only contained into the Bessel function argument; second, the approximations used for $I_0(x)$ and $\ln I_0(x)$ effectively by-pass the non linearity introduced by the logarithm.

Let's proceed by taking into account that $|\sum_{k=1}^{L}x_k e^{-j2\pi k\Delta f T}|^2$ can also be expressed as in (25), which leads to

$$\Lambda^{\mathrm{A}} = \sum_{k=1}^{L}|x_k|^2 + \frac{1}{\Delta f_{\max}}\sum_{n=0}^{L-1}\mathrm{Re}\left\{\sum_{k=n+1}^{L}x_k x_{k-n}^*\int_{-\Delta f_{\max}}^{\Delta f_{\max}}e^{-j2\pi n\Delta f T}d\Delta f\right\} \tag{44}$$

By solving the integral of the complex exponential function over a finite domain, it is a simple matter to obtain

$$\begin{aligned}\Lambda^{\mathrm{A}} \;=\; & \sum_{k=1}^{L}|x_k|^2 + 2\,\mathrm{sinc}(2\Delta f_{\max}T)\mathrm{Re}\left\{\sum_{k=2}^{L}x_k x_{k-1}^*\right\} + 2\,\mathrm{sinc}(2\cdot 2\Delta f_{\max}T)\mathrm{Re}\left\{\sum_{k=3}^{L}x_k x_{k-2}^*\right\} + \cdots + \\ + \;& 2\,\mathrm{sinc}(2n\Delta f_{\max}T)\mathrm{Re}\left\{\sum_{k=n+1}^{L}x_k x_{k-n}^*\right\} + \cdots + 2\,\mathrm{sinc}(2(L-1)\Delta f_{\max}T)\,\mathrm{Re}\{x_L x_1^*\}\end{aligned} \tag{45}$$

which can be expressed more concisely as

$$\Lambda^{\mathrm{A}} = \Lambda_0 + \sum_{n=1}^{L-1}\mathrm{sinc}(2n\Delta f_{\max}T)\cdot\Lambda_n^{\mathrm{A}} \tag{46}$$

where Λ_0 is again NCPDI and, introducing a nomenclature similar to the previous subsection,

$$\Lambda_n^{\mathrm{A}} = 2\mathrm{Re}\left\{\sum_{k=n+1}^{L}x_k x_{k-n}^*\right\} \qquad n\text{-Span DPDI-Real} \tag{47}$$

The subsequent average LRT is simply

$$\Lambda^{\mathrm{A}} \underset{\hat{H}_0}{\overset{\hat{H}_1}{\gtrless}} \xi \tag{48}$$

and the system implementing this test is denoted as APDI[Λ]. Its block diagram is reported in Fig. 3(b), while the block diagrams of the Λ_n^{A} terms is reported in Fig. 2(c). It can be noted that the Λ_n^{A} terms are formally similar to the Λ_n^{G} terms except for the very important fact that the real part is taken instead of the module, and therefore we denote them as n-Span DPDI-Real (compare with [12]). Furthermore, each Λ_n^{A} term is now weighted by a coefficient equal to $\mathrm{sinc}(2n\Delta f_{\max}T)$. It is necessary to note that, whenever $\Delta f_{\max}$ is comparable to $1/2T$, this weighting coefficient is small and possibly negative. Therefore, the considerations that led us to truncate GPDI[Λ] are ever more applicable here, and can actually lead to the use of a smaller number of terms in the sum. Similarly to GPDI, we thus introduce the truncated cases APDI[$\Lambda(m)$], with $m < L$. A practical solution can be obtained by arresting the sum at the second term only, i.e. considering the LR

$$\Lambda^{\mathrm{A}}(2) = \Lambda_0 + \mathrm{sinc}(2\Delta f_{\max}T)\ \Lambda_1^{\mathrm{A}} \tag{49}$$

and the corresponding APDI[$\Lambda(2)$] system. On the other hand, when $\Delta f_{\max}$ is small with respect to $1/2T$, the weighting coefficients are close to 1 and the real part produces much less noise enhancement than the module operation. Therefore, we can expect APDI[Λ] to outperform GPDI[Λ] for small frequency errors. The final trade-off between the two depends upon the channel conditions at hand.

IV. Performance Analysis

Even though the coherent correlation outputs x_k are complex Gaussian variates, the exact analysis of the proposed GPDI and APDI schemes is a formidable task, due to three concomitant facts:

i) several Gaussian terms are cross multiplied and then summed; the distribution of the product of non-zero mean Gaussian variates is not known in closed-form;

ii) within the generic Λ_n^{G} (and Λ_n^{A}), there may exist cross-correlations between the terms in the sum;

iii) the Λ_n^{G}, Λ_m^{G} couples (and Λ_n^{A}, Λ_m^{A}) are not mutually statistically independent for generic n and m values.

This section attempts to face this complex analytical characterization problem, starting from the single n-Span differential terms, and then discussing the general GPDI[Λ] and APDI[Λ] cases. Performance is in terms of correct detection and false alarm probabilities, defined respectively as

$$P_d = \int_{\xi}^{\infty} p_{\Lambda^i|H_1}(\Lambda)d\Lambda, \qquad P_{fa} = \int_{\xi}^{\infty} p_{\Lambda^i|H_0}(\Lambda)d\Lambda \tag{50}$$

where $p_{\Lambda^i|H_1}(\Lambda)$ and $p_{\Lambda^i|H_0}(\Lambda)$ are the pdf of the detection variable Λ^i, $i = \mathrm{G}, A$, under H_1 and H_0, respectively. Alternatively, the missed detection probability, $P_{md} = 1 - P_d$, can be used in place of the correct detection probability.

A. Λ_n^{G} and Λ_n^{A} analysis

The case for Λ_0, i.e. the analysis of NCPDI, is known from the literature (see for example [11]). Here the focus is on the case $n \geq 1$. It can be observed that the value $n = (L-1)/2$ corresponds to the frontier between statistical dependence and independence within $\Lambda_n^{\mathrm{G},A}$. Namely, whenever $\lceil (L-1)/2 \rceil \leq n < L-1$, Λ_n^{G} and Λ_n^{A} are composed by statistically independent products, while when $1 \leq n < \lfloor (L-1)/2 \rfloor$ cross-correlations between the composing products are present. In the following, we identify as *no cross-correlations* (NCC) and *cross-correlations* (CC) these two cases, respectively.

Let's start by considering the GPDI generic term Λ_n^{G}. We can rewrite $\Lambda_n^{\mathrm{G}} = 2\sqrt{z_p^2 + z_q^2}$, with $z_p = \mathrm{Re}\left\{\sum_{k=n+1}^{L} x_k x_{k-n}^*\right\}$ and $z_q = \mathrm{Im}\left\{\sum_{k=n+1}^{L} x_k x_{k-n}^*\right\}$. Notice that z_p also corresponds to one half of the APDI Λ_n^{A} term. Each z_p and z_q is composed by the sum of $N = L-n$ complex terms, i.e. $2N$ real components. Letting $x_k = x_k^p + j x_k^q$, we can specialize $z_p = \sum_{k=n+1}^{L} \left(x_k^p x_{k-n}^p + x_k^q x_{k-n}^q\right)$, and $z_q = \sum_{k=n+1}^{L} \left(x_k^q x_{k-n}^p - x_k^p x_{k-n}^q\right)$. To proceed with the analysis, it is useful to extract the mean statistical values from the variables under study. Let $x_k^{p,0} = x_k^p - \mu_k^p \sim \mathcal{N}(0, \sigma^2)$, and $x_k^{q,0} = x_k^q - \mu_k^q \sim \mathcal{N}(0, \sigma^2)$, being μ_k^p, and μ_k^q the mean values associated to x_k^p, and x_k^q, respectively, i.e.

$$\mu_k^p = \sqrt{PT}\,\mathrm{sinc}(\Delta f T)\cos(2\pi k \Delta f T + \theta), \qquad \mu_k^q = \sqrt{PT}\,\mathrm{sinc}(\Delta f T)\sin(2\pi k \Delta f T + \theta) \tag{51}$$

Thus, z_p can be written as the sum of a zero-mean term, v_p, and a non zero-mean term, w_p, i.e. $z_p = v_p + w_p$, with

$$v_p = \sum_{k=n+1}^{L} \left(x_k^{p,0} x_{k-n}^{p,0} + x_k^{q,0} x_{k-n}^{q,0}\right) \tag{52}$$

$$w_p = \sum_{k=n+1}^{L} \left(x_k^{p,0} \mu_{k-n}^p + x_k^{q,0} \mu_{k-n}^q + \mu_k^p x_{k-n}^{p,0} + \mu_k^q x_{k-n}^{q,0} + \mu_k^p \mu_{k-n}^p + \mu_k^q \mu_{k-n}^q\right) \tag{53}$$

Obviously, $w_p = 0$ under H_0. A similar approach is also followed for $z_q = v_q + w_q$.

When the NCC case is considered, v_p and v_q are the sum of $2N$ independent products of real zero-mean Gaussian rv's. Interestingly, their pdf can be found in closed-form, and with the help of [19], [20] we can write

$$p_v(v) = \frac{|v|^{N-\frac{1}{2}} K_{N-\frac{1}{2}}\left(\frac{|v|}{\sigma^2}\right)}{\sqrt{\pi}\,\Gamma(N)\,2^{N-\frac{1}{2}}\sigma^{2N+1}} = H(N)|v|^{N-1} e^{-|v|/\sigma^2} \sum_{m=0}^{N-1} H_m(N)|v|^{-m} \tag{54}$$

where $K_\nu(z)$ is the modified Bessel function of the second kind of order ν, $\Gamma(z)$ is the Gamma function, and

$$H(k) = \frac{1}{(k-1)!2^k\sigma^{2k}} \qquad H_m(k) = \left((k-1)+\frac{1}{2},m\right)\left(\frac{2}{\sigma^2}\right)^{-m} \tag{55}$$

being $(k+\frac{1}{2},m) = \frac{(k+m)!}{m!\,\Gamma(k-m+1)} = \frac{(k+m)!}{m!\,(k-m)!}$ the Henkel symbol [21]. The corresponding complementary cumulative distribution function (cdf) can then be shown to be equal to

$$F_{c,v}(v) = \begin{cases} v<0: & H(N)\sum\limits_{m=0}^{N-1} H_m(N)\,\sigma^{2(N-m)}\left\{\gamma\left(N-m,-\frac{v}{\sigma^2}\right)+(N-m-1)!)\right\} \\ v\geq 0: & H(N)\sum\limits_{m=0}^{N-1} H_m(N)\,\sigma^{2(N-m)}\,\Gamma\left(N-m,\frac{v}{\sigma^2}\right) \end{cases} \tag{56}$$

where $\Gamma(a,b)$ and $\gamma(a,b)$ are the dual incomplete gamma functions defined as, respectively [20]

$$\Gamma(k,z) = \int_z^\infty e^{-t}t^{k-1}dt, \qquad \gamma(k,z) = \int_0^z e^{-t}t^{k-1}dt, \quad Re\{k\}>0 \tag{57}$$

Under H_1, the characterization of w_p and w_q is also required. These terms are simply Gaussian rv's: $w_p \sim \mathcal{N}(M_p,\sigma_w^2)$ and $w_q \sim \mathcal{N}(M_q,\sigma_w^2)$, with

$$\begin{aligned} M_p &= \sum_{k=n+1}^{L}(\mu_k^p\mu_{k-n}^p+\mu_k^q\mu_{k-n}^q), \quad M_q = \sum_{k=n+1}^{L}(\mu_k^q\mu_{k-n}^p-\mu_k^p\mu_{k-n}^q) \\ \sigma_w^2 &= \sigma^2\left[\sum_{k=1}^{N}\left((\mu_{k+n}^p)^2+(\mu_{k+n}^q)^2\right)+\sum_{k=n+1}^{L}\left((\mu_{k-n}^p)^2+(\mu_{k-n}^q)^2\right)\right] \end{aligned}$$

The terms v_p and w_p are statistically uncorrelated, as well as v_q and w_q. However, due to the non-Gaussian distribution of v_p and v_q, statistical independence is not necessarily implied. Neglecting the possible statistical dependence, the approximate pdf of z_p can be computed through the convolution integral. A significant effort in calculus leads to

$$\begin{aligned} p_{z_p}(z) &= C\exp\left\{-\frac{(z-M_p)^2}{2\sigma_w^2}\right\}\sum_{m=0}^{N-1}H_m(N)\,\sigma_w^{N-m}(N-m-1)! \\ &\quad\left[\exp\left\{\frac{\sigma_w^2}{4}\left(\frac{1}{\sigma^2}-\frac{z-M_p}{\sigma_w^2}\right)^2\right\}D_{m-N}\left(\sigma_w\left(\frac{1}{\sigma^2}-\frac{z-M_p}{\sigma_w^2}\right)\right)+\right. \\ &\quad\left.+\exp\left\{\frac{\sigma_w^2}{4}\left(\frac{1}{\sigma^2}+\frac{z-M_p}{\sigma_w^2}\right)^2\right\}D_{m-N}\left(\sigma_w\left(\frac{1}{\sigma^2}+\frac{z-M_p}{\sigma_w^2}\right)\right)\right] \end{aligned} \tag{58}$$

and similarly for $p_{z_q}(z)$ replacing M_p with M_q, where $D_p(z)$ is the parabolic cylinder function [20]

$$D_p(z) = 2^{\frac{1}{4}+\frac{p}{2}}W_{\frac{1}{4}+\frac{p}{2},-\frac{1}{4}}\left(\frac{z^2}{2}\right)z^{-\frac{1}{2}} \tag{59}$$

where $W_{\lambda,\mu}(z)$ is the Whittaker function, and $C = 1/\sqrt{2\pi}(N-1)!\ 2^N\,\sigma_w\ \sigma^{2N}$. A further burdensome analytical effort brings us to the corresponding complementary cdf

$$\begin{aligned} F_{c,z_p}(z) \ = \ & \frac{1}{(N-1)!\,2^{N+1}} \sum_{m=0}^{N-1} 2^{-m} \frac{(N+m-1)!}{m!} \left\{ 2\,\mathrm{erfc}\left(\frac{z-M_p}{\sqrt{2}\sigma_w}\right) + \sqrt{\frac{2}{\pi}}\frac{1}{\sigma_w}\exp\left\{-\frac{(z-M_p)^2}{2\sigma_w^2}\right\} \right. \\ & \sum_{j=1}^{N-m} \frac{\sigma_w^j}{\sigma^{2(j-1)}} \left[\exp\left\{ \frac{\sigma_w^2}{4}\left(\frac{1}{\sigma^2} - \frac{z-M_p}{\sigma_w^2}\right)^2 \right\} D_{-j}\left(\sigma_w\left(\frac{1}{\sigma^2} - \frac{z-M_p}{\sigma_w^2}\right)\right) + \right. \\ & \left. \left. - \exp\left\{ \frac{\sigma_w^2}{4}\left(\frac{1}{\sigma^2} + \frac{z-M_p}{\sigma_w^2}\right)^2 \right\} D_{-j}\left(\sigma_w\left(\frac{1}{\sigma^2} + \frac{z-M_p}{\sigma_w^2}\right)\right) \right] \right\} \end{aligned} \tag{60}$$

Equations (54) and (58) are a significant result on their own, and can additionally be used to extract the exact mean and variance of z_p and z_q. In turn, these values are instrumental in the derivation of a model for $z = \sqrt{z_p^2 + z_q^2}$. Observing that z_p and z_q are the sum of a significant number of terms, we apply the central limit theorem and derive a Gaussian approximation which inherits the statistical moments and the asymptotic tail behavior. This immediately leads to a Rice/Rayleigh distribution for z under H_1/H_0, respectively. In particular, the tail behavior of the exact distribution is fundamental under H_0. In order to ensure maximal tail distribution congruence, the second central moment of the approximating Gaussian rv is obtained through a proper scaling procedure, as reported in the Appendix. Thus, under H_0, v_p and v_q are approximated by a zero-mean Gaussian rv with variance equal to $s_v\,\sigma^2_{v,NCC}$, where s_v is the scaling factor, and $\sigma^2_{v,NCC} = 2H(N)\sum_{m=0}^{N-1} H_m(N)\sigma^{2(N-m+2)}(N-m+1)!$ is the variance of the pdf (54). The generic GPDI Λ_n^{G} term is Rayleigh distributed, and if we perform detection adopting this Λ_n^{G} scheme as a stand-alone detector, the corresponding false alarm probability is

$$P_{fa}(\Lambda_n^{\mathrm{G}}, NCC) = \exp\left\{-\xi^2/8 s_v \sigma^2_{v,NCC}\right\} \tag{61}$$

In the case of H_1, the agreement in the tail distribution is obtained by direct inheritance of the first and second statistical moments from the pdf in (58), i.e. of the means M_p and M_q and of the common variance $\sigma^2_{z,NCC} = \sigma_w^2 + \sigma^2_{v,NCC}$. Thus, the generic Λ_n^{G} term is Rice distributed, and its complementary cdf (i.e. correct detection probability associated to the stand-alone detector) is

$$P_d(\Lambda_n^{\mathrm{G}}, NCC) = Q\left(\frac{\eta}{\sigma_{z,NCC}}, \frac{\xi}{2\sigma_{z,NCC}}\right) \tag{62}$$

where $\eta = \sqrt{M_p^2 + M_q^2}$, and $Q(a,b)$ is the Marcum Q function.

When cross-correlations are present (CC case), we split the rv v_p (and v_q) into two parts, each one containing statistically independent products. In particular, we subdivide it into an odd, v_p^{O}, and an even sub-term, v_p^{E}, by alternately considering the sum of groups of n consecutive products; more

formally, $v_p^{\mathrm{O}} = \sum_{k\in I_{\mathrm{O}}}[x_k^{p,0}(x_{k-n}^{p,0})^* + x_k^{q,0}(x_{k-n}^{q,0})^*]$ and $v_p^{\mathrm{E}} = \sum_{k\in I_{\mathrm{E}}}[x_k^{p,0}(x_{k-n}^{p,0})^* + x_k^{q,0}(x_{k-n}^{q,0})^*]$, being $I_{\mathrm{O}} = \{n+1,\ldots,2n,3n+1,\ldots,4n,\ldots\}$ and $I_{\mathrm{E}} = \{2n+1,\ldots,3n,4n+1,\ldots,5n,\ldots\}$, with $k \leq L$. Indicating with N_{O} and N_{E} the cardinality of I_{O} and I_{E}, respectively, it can be shown that $N_{\mathrm{O}} = \left\lceil \frac{1}{2}\left\lfloor \frac{N}{n} \right\rfloor \right\rceil n + \mathrm{mod}(N,n)$ and $N_{\mathrm{E}} = N - N_O$, where mod(h,k) indicates the remainder of the integer division of h by k. Thus,

$$z_p = v_p + w_p = v_p^{\mathrm{O}} + v_p^{\mathrm{E}} + w_p \tag{63}$$

A similar notation holds for z_q. The terms v_p^{O} and v_p^{E} (and similarly v_q^{O} and v_q^{E}) are thus distributed as in (54), by replacing N with N_{O} and N_{E}, respectively. Similarly to the NCC case, the corresponding variances $\sigma_{v,\mathrm{O}}^2$ and $\sigma_{v,\mathrm{E}}^2$ are equal to $\sigma_{v,NCC}^2$, again replacing N with N_{O} and N_{E}. To proceed in the characterization, the Gaussian approximation is introduced for both the odd and the even rv's, according to the tail fitting algorithm reported in the Appendix. Thus, we assume $v_p^{\mathrm{O}} \sim \mathcal{N}(0, s_v^{\mathrm{O}}\ \sigma_{v,\mathrm{O}}^2)$ and $v_p^{\mathrm{E}} \sim \mathcal{N}(0, s_v^{\mathrm{E}}\ \sigma_{v,\mathrm{E}}^2)$, being s_v^{O} and s_v^{E} the corresponding scaling parameters. Now, the fundamental observation is that v_p^{O} and v_p^{E} are uncorrelated, so that v_p is the sum of two uncorrelated Gaussian rv's, and is therefore Gaussian with zero-mean and variance $\sigma_{v,CC}^2 = s_v^{\mathrm{O}}\ \sigma_{v,\mathrm{O}}^2 + s_v^{\mathrm{E}}\ \sigma_{v,\mathrm{E}}^2$. Similarly, v_q is a zero-mean Gaussian variate with same variance. Under H_0, the GPDI Λ_n^{G} term is thus distributed as a Rayleigh variate with corresponding false alarm probability given by eq. (61) with $\sigma_{v,CC}^2$ in place of $s_v\sigma_{v,NCC}^2$. Under H_1, w_p and w_q are also present, and $z_p \sim \mathcal{N}(M_p, \sigma_{z,CC}^2)$, $z_q \sim \mathcal{N}(M_q, \sigma_{z,CC}^2)$, where $\sigma_{z,CC}^2 = \sigma_{v,CC}^2 + \sigma_w^2$. The GPDI term Λ_n^{G} is thus distributed as a Rice rv with corresponding correct detection probability given by eq. (62) with $\sigma_{z,CC}$ in place of $\sigma_{z,NCC}$.

Considering the generic APDI n-Span term, we can observe that $\Lambda_n^{\mathrm{A}} = 2z_p$, where z_p has already been characterized. When NCC is considered, under H_0 the complementary cdf of z_p is given by (56) and the false alarm probability associated to Λ_n^{A} is straightforward, i.e.

$$P_{fa}(\Lambda_n^{\mathrm{A}}, NCC) = F_{c,v}(\xi/2) \tag{64}$$

As shown later, this exact expression provides very good match with numerical simulation results. Under H_1, we obtain for z_p the complementary cdf in (60). The missed detection probability associated to Λ_n^{A} is then simply

$$P_{md}(\Lambda_n^{\mathrm{A}}, NCC) = F_{c,z_p}(\xi/2) \tag{65}$$

When the CC case is considered, under H_0 z_p is equal to $v_p \sim \mathcal{N}(0, \sigma_{v,CC}^2)$. Thus, the false alarm probability is simply

$$P_{fa}(\Lambda_n^{\mathrm{A}}, CC) = \frac{1}{2}\ \mathrm{erfc}\left(\frac{\xi}{\sqrt{2}\sigma_{v,CC}}\right) \tag{66}$$

Under H_1, $z_p \mathcal{N}(M_p, \sigma^2_{z,CC})$. Therefore, the missed detection probability is simply given by

$$P_{md}(\Lambda_n^{\mathrm{A}}, CC) = \frac{1}{2} \operatorname{erfc}\left(\frac{\xi - M_p}{\sqrt{2}\sigma_{z,CC}}\right) \tag{67}$$

The validation of the Λ_n^{G} and Λ_n^{A} analysis is presented respectively in Figs. 4 and 5, for an NCC case (n=10), and a CC case (n=2), with $M = 10$, $L = 16$, and $E_s/N_0 = 2$dB. By observing these figures, we can conclude that the proposed characterizations for the single GPDI and APDI terms lead to good match with numerical simulations. Obviously, the exact expressions for APDI NCC under H_0 yields a perfect match.

Notice that the DPDI and DPDI-Real analysis can be derived as a particular case from the aforementioned considerations by setting n=1. A different approach to the exact characterization of DPDI and DPDI-Real is provided in [15].

B. GPDI[Λ] and APDI[Λ] analysis

The overall analytical characterization of the total Λ variable is a formidable and open problem. For GPDI[Λ] we have to model the rv obtained by summing NCPDI and all Λ_n^{G} terms, both with and without cross-correlations inside, taking into account their mutual statistical dependence. Even if we assumed to neglect this mutual interdependence, we would still have to close the convolution integral between a central/non-central chi-square distribution (given by NCPDI) and $L-1$ Rayleigh/Rice distributions for H_0/H_1. The result is not known in closed-form. The situation is even more difficult for APDI[Λ], where under the assumption of neglecting the statistical interdependence, we would have to convolve a central/non-central chi-square distribution with $L-1$ pdf's of the type (54)/(58) for H_0/H_1.

Both of these problems are left for future research efforts, and we resort to numerical simulations in the next section.

V. NUMERICAL RESULTS

In the following, simulation results are reported for GPDI and APDI in AWGN in terms of ROCs, i.e., missed detection probability versus false alarm probability. As observed before, the APDI scheme derivation is obtained under the assumption of a uniformly distributed frequency error, but the experienced frequency offset is in practice an unknown fixed parameter. It is essential that numerical simulations correctly reproduce this modelling mismatch to obtain a realistic evaluation of the APDI performance.

Fig. 6 shows the performance comparison between NCPDI, DPDI, and GPDI, for $M = 10$, $L = 16$, $E_s/N_0 = 2$dB, and $\Delta f T = 0.2$. In addition to the case of GPDI[Λ], several truncated schemes GPDI[$\Lambda(m)$] are also considered.

Observation 1: There exists a crossing point between the ROCs of the single NCPDI and DPDI terms. DPDI outperforms NCPDI for small required P_{fa}, while the opposite holds for small required P_{md}. Because the former case is more frequent in practice, it can be stated that DPDI is generally preferable to NCPDI.

Observation 2: GPDI[$\Lambda(2)$] consistently outperforms both NCPDI and DPDI.

Observation 3: The GPDI[$\Lambda(m)$] performance improves monotonically up until the total GPDI[Λ] scheme. However, the incremental improvement becomes smaller for larger m, and a practical saturation trend can be observed.

In the specific case under evaluation, m=12 has practically the same performance as GPDI[Λ] with 16 terms. The justification of this saturation comes from Fig. 7, which shows the single term performance of all composing elements. As expected, the strongest contributions come from lower n values, while large n produces weak terms.

Fig. 8 illustrates the comparison between APDI and GPDI for an experienced fixed frequency error of $\Delta fT = 0.2$, under the specification of a maximum normalized frequency offset of 0.25. In other words, the frequency error is averaged over the range [-0.25, 0.25] for APDI. Due to the APDI model mismatch, GPDI turns out to be more robust. The APDI solution can achieve slightly better performance than DPDI if a large number of terms are summed. APDI[$\Lambda(2)$] and APDI[$\Lambda(4)$] are worse than simple DPDI. APDI[$\Lambda(2)$] in particular approaches NCPDI. Increasing m, the APDI performance saturates onto GPDI[$\Lambda(2)$].

Observation 4: The APDI strategy is much weaker than GPDI with a large frequency error.

However, if we consider a scenario with a reduced frequency offset, the GPDI vs. APDI comparison must be completely revisited. For example, assuming $\Delta f_{\max} T = 0.05$, and the experienced frequency error equal to $\Delta f_{\max}$, we obtain the performance reported in Fig. 9. In this case, GPDI has better performance than before due to the reduced frequency degradation, and again GPDI[Λ] outperforms GPDI[$\Lambda(2)$], NCPDI, and DPDI. More importantly,

Observation 5: For moderate to small frequency offsets, APDI[$\Lambda(2)$] improves consistently its performance with respect to NCPDI, DPDI, and also GPDI[$\Lambda(2)$].

This is mainly due to the increase of the weighting coefficients $\mathrm{sinc}(2n\Delta f_{\max} T)$ with lower values of $\Delta f_{\max}$. Even more striking is the fact that APDI[$\Lambda(4)$] goes all the way to outperform even GPDI[Λ].

Observation 6: The trend for APDI[$\Lambda(m)$] is not in general monotonic with increasing m.

In fact, $m = 8, 12$ and the total APDI[Λ] provide worse and worse performance. This behavior is due to the fact that the single APDI terms can become negative for large values of m. In essence, truncation

for APDI is a matter of performance and not just complexity.

By further reducing the maximum frequency error, e.g. $\Delta f_{\max} T = 0.005$, again assumed to be equal to the experienced frequency offset, we obtain the performance in Fig. 10.

Observation 7: For small frequency offsets, all APDI terms outperform GPDI[Λ], because all APDI weighting coefficients are close to 1, and the noise enhancement is minimal. In this case, the APDI ROCs improve monotonically as m increases.

Finally note that even the least complex APDI[$\Lambda(2)$] outperforms GPDI[Λ] in this case.

VI. Discussion and Conclusions

This paper tackles the problem of code acquisition in the presence of phase and frequency uncertainty. Differently from the pragmatic approach typically adopted in the literature to limit the degradation induced by the frequency offset (NCPDI and DPDI solutions), this paper derives the quasi-optimal PDI scheme by means of a theoretical investigation. Two different strategies are adopted, namely the generalized and average likelihood ratio tests, yielding the GPDI and APDI schemes, respectively. An approximate analytical characterization has been presented for n-Span DPDI and DPDI-Real terms. A thorough numerical investigation in AWGN reveals a consistent performance improvement of the proposed solutions with respect to NCPDI and DPDI, and allows to optimize the performance/complexity trade-off. In particular, the additional complexity related to the introduction of GPDI and APDI can be limited by selecting a properly truncated version. Further, the selection between GPDI and APDI should be driven by the specific maximum frequency offset characterizing the application. In fact, with small offsets APDI is the best solution due to its reduced noise enhancement; instead, in the presence of large frequency errors GPDI outperforms all other alternatives, and reveals itself as the best solution.

Appendix

This Appendix describes a tail fitting procedure to scale the variance of the Gaussian approximation for the exact distribution given in (54). Fitting the tails is the most important objective in threshold crossing problems. To this aim, the fitting algorithm employs the exact complementary cdf of v_p and v_q, i.e. (56) for $v \geq 0$, and searches for the value $v = \bar{v}$ for which $F_{c,v}(\bar{v}) = \frac{1}{2} \operatorname{erfc}\left(\frac{4}{\sqrt{2}}\right) = 3 \cdot 10^{-5}$, i.e., the value assumed by the Gaussian complementary cdf at a distance of 4 times the standard deviation from its mean value. Imposing $\bar{v} = 4\sqrt{s_v}\sigma_v$ yields

$$s_v = \frac{\bar{v}^2}{16\sigma_v^2} \tag{68}$$

Evidently, this procedure provides its best accuracy for probabilities in the order of 10^{-5}. If lower probabilities are of interest, the same fitting procedure in principle can be repeated, simply changing the target $F_{c,v}(\bar{v})$ value.

ACKNOWLEDGEMENT

The Authors are grateful to Dr. Andrew J. Viterbi for the very helpful discussions and encouragement. This work has been supported in part by the EC-IST MAESTRO project (IST-2003-507023) and partially presented in [22], [23], [24].

REFERENCES

[1] R.A. Scholtz, "The Origins of Spread-Spectrum Communications," *IEEE Trans. Comm.*, vol. 30, no. 5, pp. 822–854, May 1982.

[2] R.L. Pickholtz, D.L. Schilling, and L.B. Milstein, "Theory of Spread-Spectrum Communications - A Tutorial," *IEEE Trans. Comm.*, vol. 30, no. 5, pp. 855–884, May 1982.

[3] M.K. Simon, J.K. Omura, R.A. Scholtz, and B.K. Levitt, *Spread Spectrum Communications Handbook*, Mc Graw Hill, Inc., 1994.

[4] A. Polydoros and C.L. Weber, "A Unified Approach to Serial Search Spread Spectrum Code Acquisition - Part I: General Theory," *IEEE Trans. Comm.*, vol. 32, no. 5, pp. 542–549, May 1984.

[5] G.E. Corazza, C. Caini, A. Vanelli-Coralli, and A. Polydoros, "DS-CDMA Code Acquisition in the Presence of Correlated Fading - Part I: Theoretical Aspects," *IEEE Trans. Comm.*, vol. 52, no. 7, pp. 1160 – 1168, July 2004.

[6] H. L. Van Trees, *Detection, Estimation, and Modulation Theory. Part I: Detection, Estimation, and Linear Modulation Theory*, John Wiley and Sons, Inc., New York, 1968.

[7] D.E. Cartier, "Partial Correlation Properties of Pseudonoise (PN) Codes in Noncoherent Synchronization/Detection Schemes," *IEEE Trans. Comm.*, vol. 24, no. 8, pp. 898–903, Aug. 1976.

[8] J. Diez, C. Pantaleon, L. Vielva, I. Santamaria, and J. Ibanez, "A Simple Expression for the Optimization of Spread-Spectrum Code Acquisition Detectors in the Presence of Carrier-Frequency Offset," *IEEE Trans. Comm.*, vol. 52, no. 4, pp. 550–552, Apr. 2004.

[9] G.E. Corazza, R. Pedone, and M. Villanti, "Frame Acquisition for Continuous and Discontinuous Transmission in the Forward Link of Ka-band Satellite Systems," *EMPS 2004 6th European Workshop on Mobile/Personal Satcoms and ASMS 2004 2nd Advanced Satellite Mobile Systems Conference*, ESA-ESTEC, Noordwijk, The Netherlands, 21-22 Sep., pp. 211–218, 2004.

[10] G.E. Corazza, R. Pedone, and M. Villanti, "MAX Strategy for Burst Frame Acquisition in Ka-band Satellite Systems," *10th Ka and Broadband Communications Conference*, Vicenza, Italy, 30 Sep.-2 Oct. , pp. 261–268, 2004.

[11] A.J. Viterbi, *CDMA, Principles of Spread Spectrum Communications*, Addison-Wesley Wireless Communications Series. Addison-Wesley Publishing Company, April 1995.

[12] G.E. Corazza, P. Salmi, A. Vanelli-Coralli, and M. Villanti, "Differential Post Detection Integration Technique in the Return Link of Satellite CDMA Systems," *IEEE ISSSTA 2002, 7th International Symposium on Spread Spectrum Techniques and Applications Conference*, Czech Republic, 2-5 Sep., pp. 233–237, 2002.

[13] G.E. Corazza, P. Salmi, A. Vanelli-Coralli, and M. Villanti, "Differential and Non-Coherent Post Detection Integration Techniques for the Return Link of Satellite W-CDMA Systems," *IEEE PIMRC02, 13th IEEE International Symposium on Personal, Indoor and Mobile Radio Communications*, Lisbon, Portugal, 15-18 Sep., pp. 300–304, 2002.

[14] O. Shin and K.B. Lee, "Differentially Coherent Combining for Double-Dwell Code Acquisition in DS-CDMA Systems," *IEEE Trans. Comm.*, vol. 51, no. 7, pp. 1046–1050, Jul. 2003.

[15] M. Villanti, P. Salmi, and G.E. Corazza, "Differential Post-Detection Integration Techniques for Robust Code Acquisition," *to be submitted to IEEE Trans. Comm.*, 2004.

[16] ETSI EN 302 307 V1.1.1 (2004-01), Digital Video Broadcasting (DVB) - Second generation framing structure, channel coding and modulation systems for Broadcasting, Interactive Services, News Gathering and other broadband satellite applications, 2004.

[17] R. Pedone, "Likelihood Ratio Testing for Post Detection Integration," Ph.D. Thesis, in preparation.

[18] Z.Y. Choi and Y.H. Lee, "Frame Synchronization in the Presence of Frequency Offset," *IEEE Trans. Comm.*, vol. 50, no. 7, pp. 1062–1065, Jul. 2002.

[19] K.S. Miller, *Multidimensional Gaussian Distributions*, The SIAM Series in Applied Mathematics, R.F. Drenick and H. Hochstadt, Editors. John Wiley and Sons, Inc., New York, 1964.

[20] I.S. Gradshteyn and I.M. Ryzhik, *Table of Integrals, Series, and Products*, Academic Press, Inc., New York, 1973.

[21] M. Abramowitz and I.A. Stegun, *Handbook of Mathematical Functions with Formulas, Graphs, and Mathematical Tables*, Dover Publicatipns, Inc., New York.

[22] G.E. Corazza and R. Pedone, "Maximum Likelihood Post Detection Integration Methods for Satellite Mobile Systems," *IEEE ICT 2003, Intern. Conf. on Telecommunications*, 23 Feb.-1 Mar. 2003, Papeete, Tahiti, French Polynesia, vol. 2, pp. 1601–1604, 2003.

[23] G.E. Corazza and R. Pedone, "Maximum Likelihood Post Detection Integration Methods for Spread Spectrum Systems," *IEEE WCNC 2003, Wireless Communications and Networking Conference*, 16-20 Mar. 2003, New Orleans, LA, USA, pp. 227–232, 2003.

[24] G.E. Corazza and R. Pedone, "Generalized and Average Post Detection Integration Methods for Code Acquisition," *IEEEE ISSSTA 2004, International Symposium on Spread Spectrum Techniques and Applications*, 30 Aug.-2 Sep., Sydney, Australia, pp. 207–211, 2004.

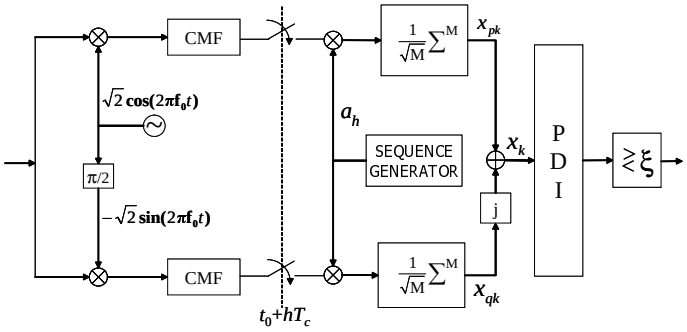

Fig. 1. General system block diagram

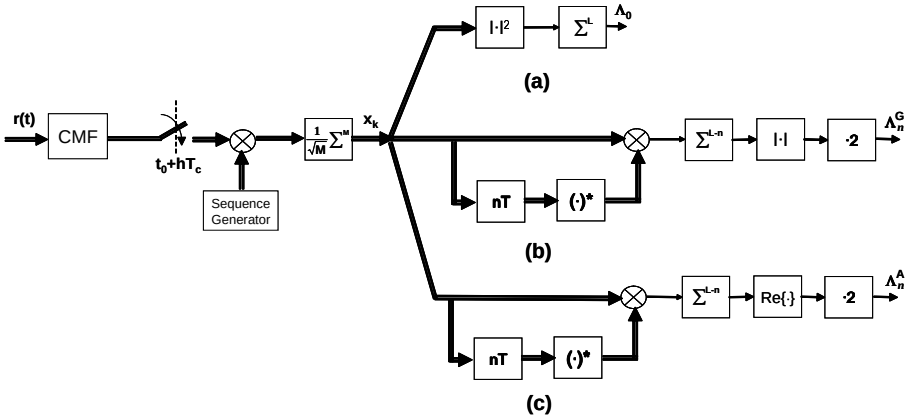

Fig. 2. Block diagrams for NCPDI (a), n-Span DPDI (b), and n-Span DPDI-Real (c)

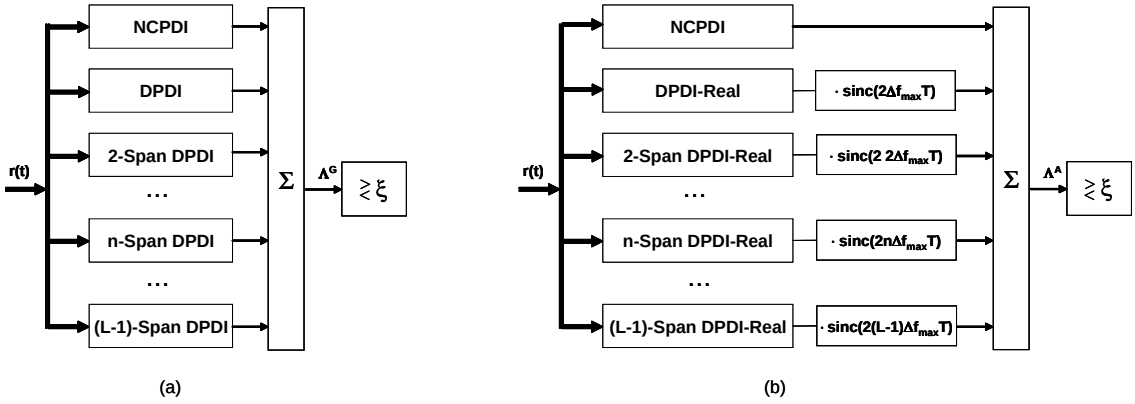

Fig. 3. Block diagrams for GPDI[Λ] (a), and APDI[Λ] (b)

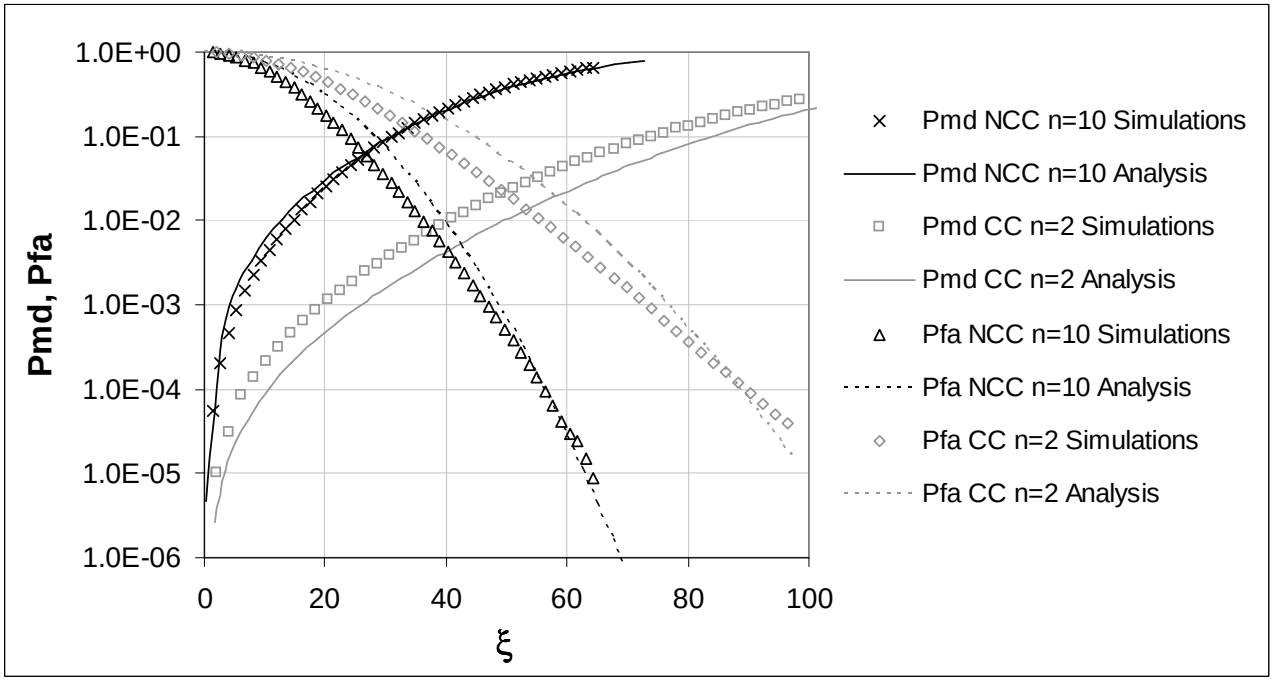

Fig. 4. Analytical model validation for GPDI Λ_n^{G} terms, M=10, L=16, $E_s/N_0 = 2$dB, $\Delta fT = 0.2$. Tail fitting parameters: s_v=1.43, s_v^{O}=1.34, s_v^{E}=1.78

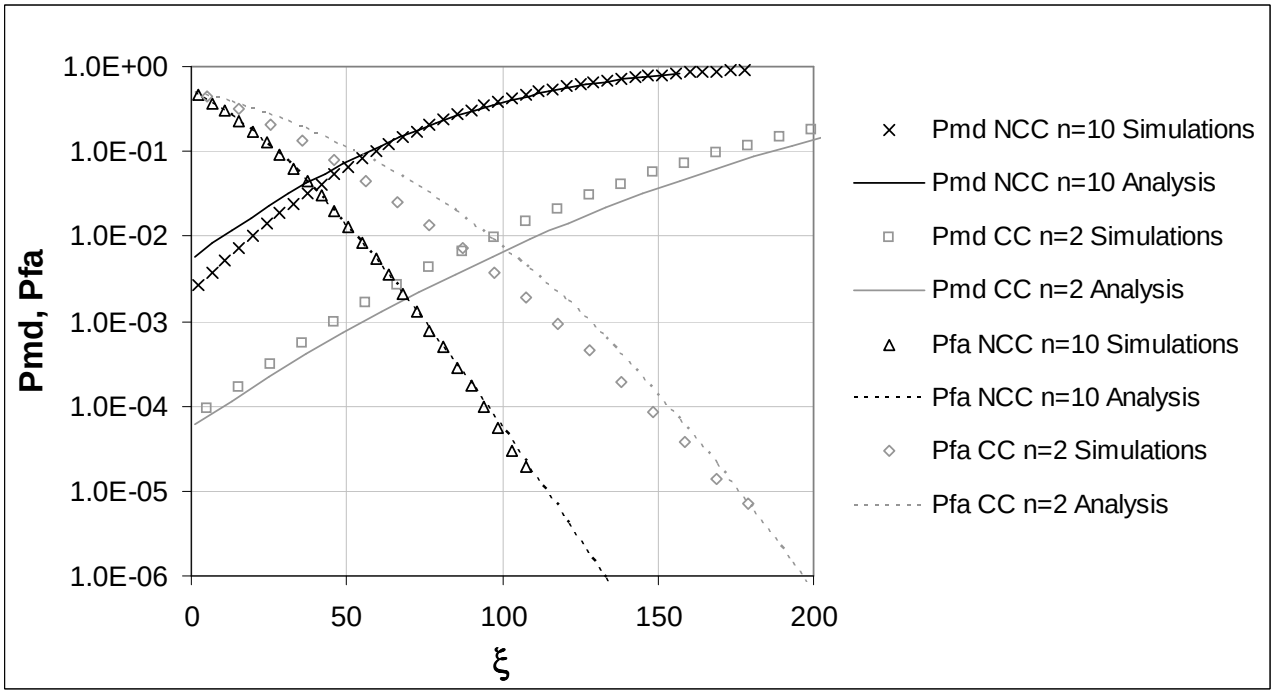

Fig. 5. Analytical model validation for APDI Λ_n^{A} terms, M=10, L=16, $E_s/N_0 = 2$dB, $\Delta fT = 0.005$, Tail fitting parameters: s_v=1.43, s_v^{O}=1.34, s_v^{E}=1.78

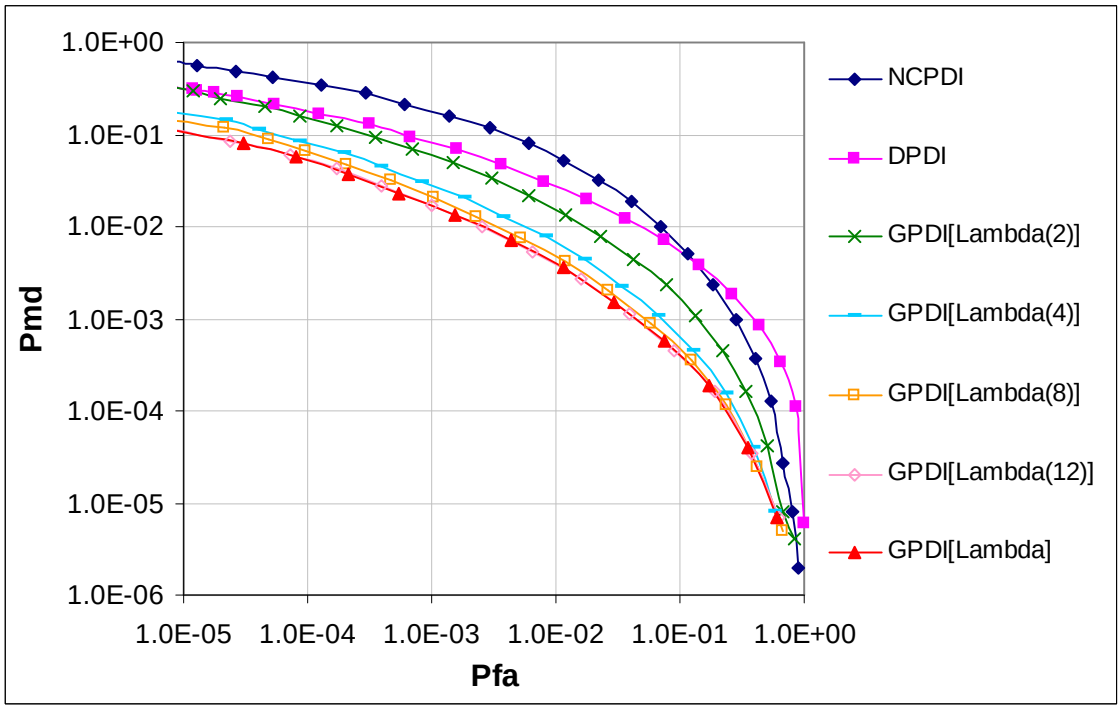

Fig. 6. Comparison between NCPDI, DPDI, and GPDI. M=10, L=16, $E_s/N_0 = 2$dB, $\Delta fT = 0.2$

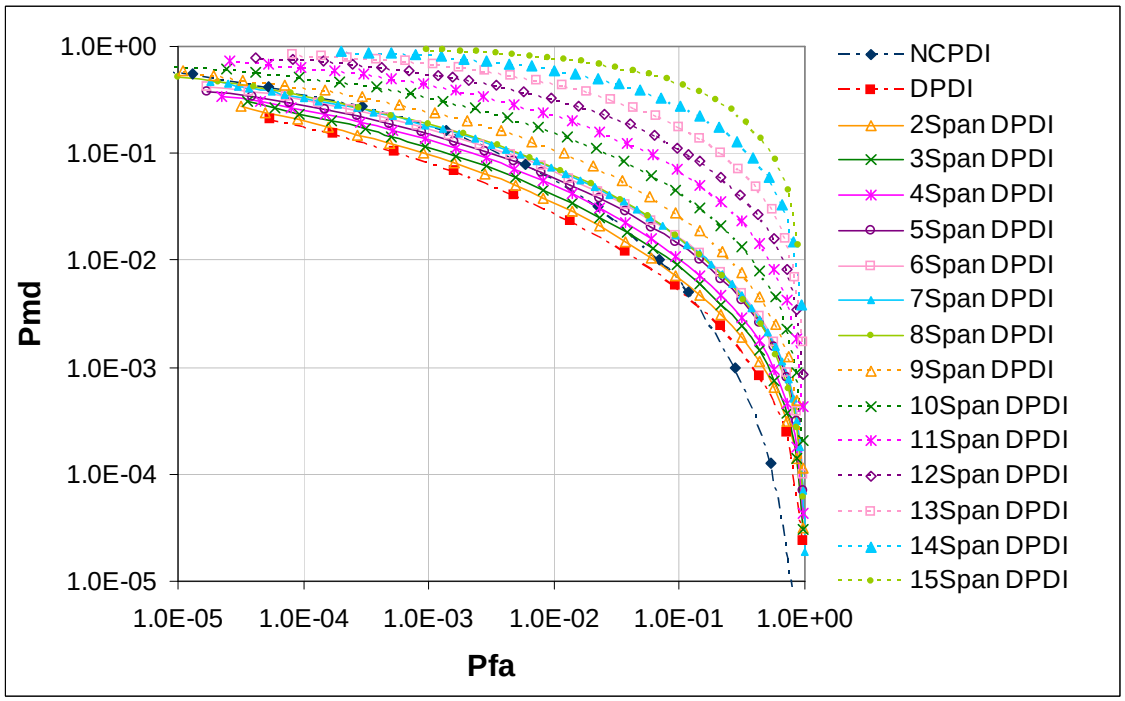

Fig. 7. Comparison between NCPDI, DPDI, and n-Span DPDI terms. M=10, L=16, $E_s/N_0 = 2$dB, $\Delta fT = 0.2$

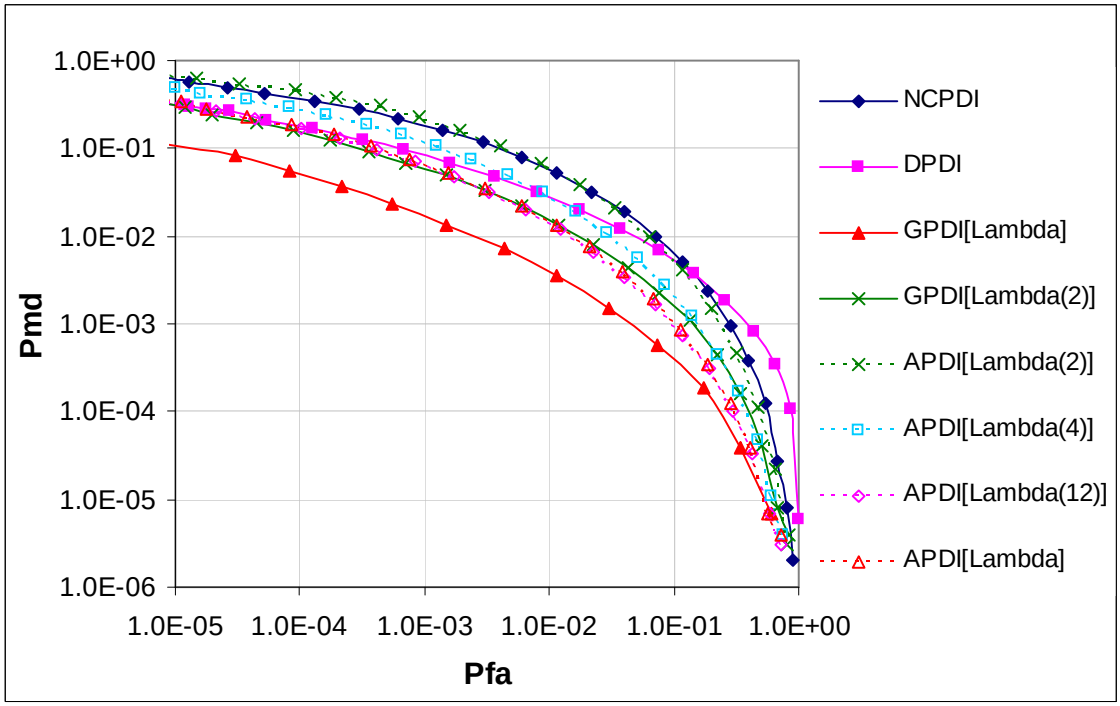

Fig. 8. Comparison between NCPDI, DPDI, GPDI and APDI. M=10, L=16, $E_s/N_0 = 2$dB, $\Delta fT = 0.2$, $\Delta f_{\max} T = 0.25$

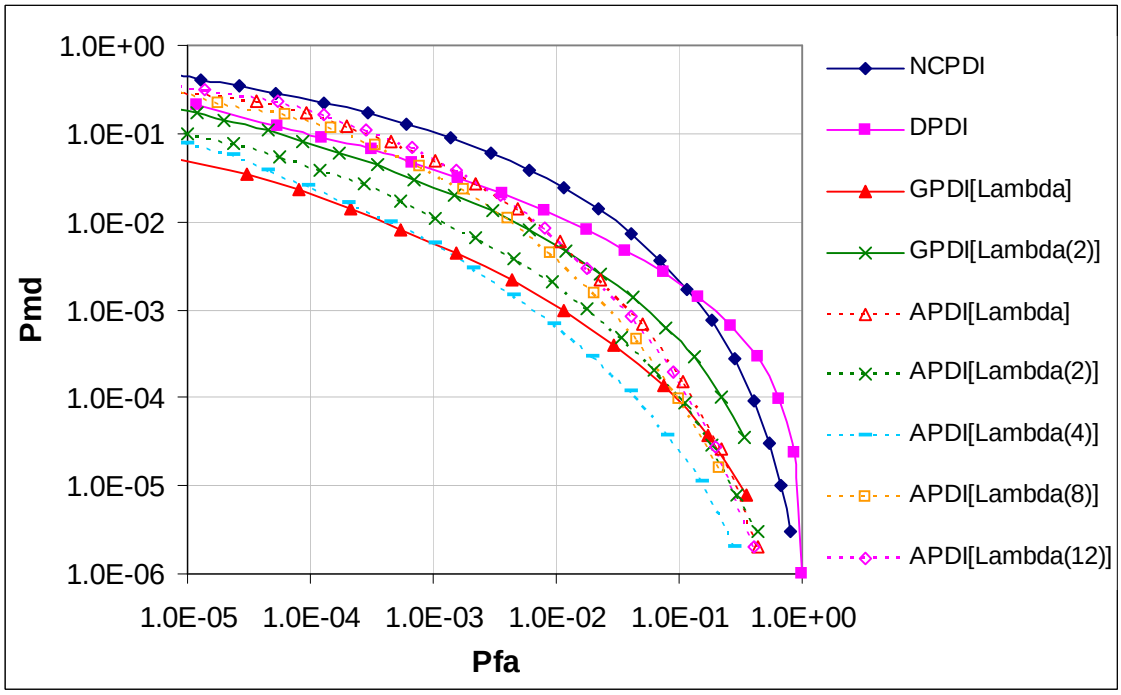

Fig. 9. Comparison between NCPDI, DPDI, GPDI and APDI. M=10, L=16, $E_s/N_0 = 2$dB, $\Delta fT = 0.05$, $\Delta f_{\max} T = 0.05$

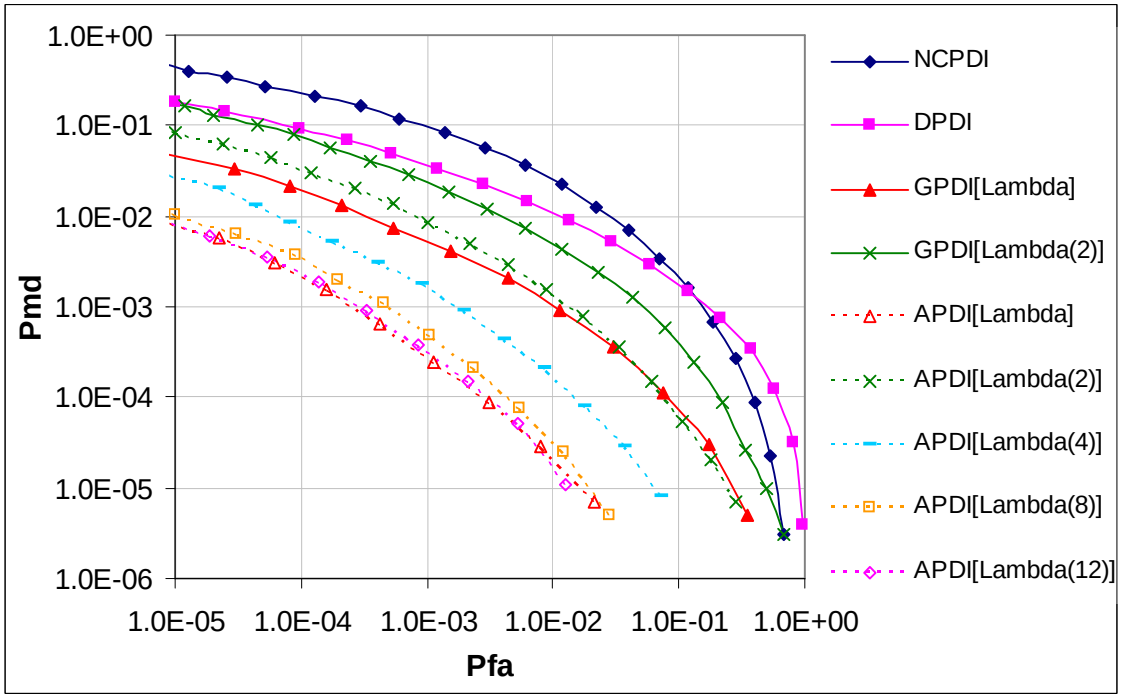

Fig. 10. Comparison between NCPDI, DPDI, GPDI and APDI. M=10, L=16, $E_s/N_0 = 2$dB, $\Delta f T = 0.005$, $\Delta f_{\max} T = 0.005$